

Content from this work may be used under the terms of the CC BY 3.0 licence (© 2018). Any distribution of this work must maintain attribution to the author(s), title of the work, publisher, and DOI.

THE PATH TO COMPACT, EFFICIENT SOLID-STATE TRANSISTOR-DRIVEN ACCELERATORS

D.C. Nguyen, C.E. Buechler, G.E. Dale, R.L. Fleming, M.A. Holloway, J.W. Lewellen, D. Patrick
 Los Alamos National Laboratory

J. Neilson, V. Dolgashev, E.N. Jongewaard, E.A. Nanni, A. Sy and S. Tantawi
 SLAC National Accelerator Laboratory

Abstract

Small, lightweight, few-MeV electron accelerators that can operate with low-voltage power sources, e.g., solid-state transistors running on 50 VDC, instead of high-voltage klystrons, will provide a new tool to enhance existing applications of accelerators as well as to initiate new ones. Recent advances in gallium nitride (GaN) semiconductor technologies [1] have resulted in a new class of high-power RF solid-state devices called high-electron mobility transistors (HEMTs). These HEMTs are capable of generating a few hundred watts at S-, C- and X-bands at 10% duty factor. We have characterized a number of GaN HEMTs and verified they have suitable RF characteristics to power accelerator cavities. We have measured energy gain as a function of RF power in a single low- β C-band cavity. The HEMT powered RF accelerators will be compact and efficient, and they can operate off the low-voltage DC power buses or batteries. These all-solid-state accelerators are also more robust, less likely to fail, and are easier to maintain and operate. In this poster, we present the design of a low- β , 5.1-GHz cavity and beam dynamics simulations showing continuous energy gain in a ten-cavity C-band prototype.

INTRODUCTION

Growing demand for small, MeV-energy electron accelerators for applications ranging from aurora mapping [2] to MRI-linac radiation therapy [3] has prompted us to replace bulky high-voltage klystrons with compact GaN HEMTs as the RF power sources for RF linac. Traditionally, solid-state RF transistors have been used in conjunction with power combiners to provide up to 100s of kW to drive high-gradient, multi-cell accelerator structures. We introduce a new approach that uses HEMTs to directly drive individual RF cavities (see Fig. 1 for the photo of a GaN HEMT and a C-band cavity).

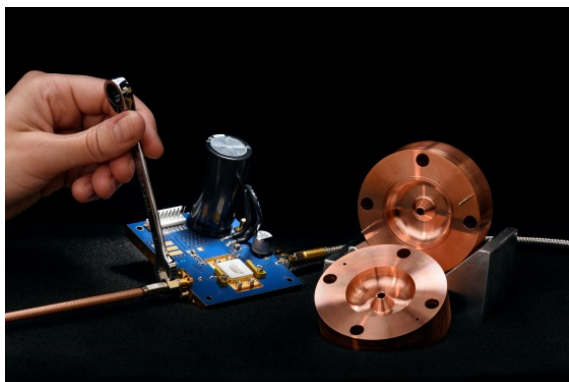


Figure 1: An HEMT with two halves of a copper cavity.

Each C-band cavity powered with 250 W of RF from a single HEMT can provide ~ 20 keV energy gain. A large number of these cavities can be strung together to provide beam energies up to a few MeV. This configuration offers the benefits of graceful degradation, in case a few HEMTs fail, low-voltage operation and variable energy output. The main challenge is the requirement for the low-level RF (LLRF) system to control the frequency, amplitude and phase of individual cavities to ensure continuous energy gain and proper focusing in the entire linac.

In this paper, we analyze the RF power aspect of HEMT-driven cavities at different frequency bands. We present initial results of the single-cavity energy gain measurements and the design of optimized low- β cavities for use in a ten-cavity prototype. The latter has been fabricated by SLAC and is being tested at LANL to study the LLRF challenges and to demonstrate continuous energy gain up to 200 keV.

HEMT FREQUENCY SELECTION

We have reviewed the literature of commercially available HEMTs at S-, C- and X-bands [3] and plotted RF power versus frequency (Fig. 2). In our solid-state RF linac design, there are no power combiners; instead, each HEMT must provide enough RF power for both the cavity field and the beam. The cavity power is given by

$$P_{cav} = \frac{|E_0 T|^2}{R_s T^2} L_{cav} \quad (1)$$

where E_0 is the accelerating gradient, T is the transit time, R_s is the cavity shunt impedance which scales with $f^{1/2}$, and L_{cav} is the cavity length which scales with $1/f$. Thus, the cavity power scales with $f^{-3/2}$ (Fig. 2, blue line).

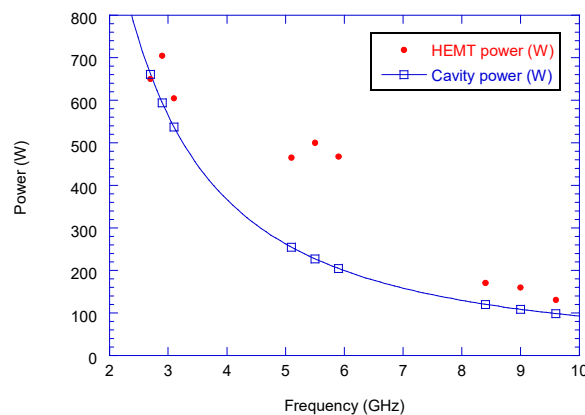


Figure 2: Plots of HEMT output power (red) and cavity power (blue) versus frequency for S-, C- and X-bands.

The difference between HEMT output power and cavity power is the RF power available for beams. C-band HEMTs are chosen because they provide at least 200 W of beam power between 5.1 and 5.9 GHz. Using 250 W for cavity power and 200 W for beam power, e.g., 20 keV and 10 mA at 10% duty factor, we calculate an RF-to-beam conversion efficiency of ~44%. Combined with the HEMT DC-to-RF conversion efficiency of ~60%, the overall wall-plug efficiency is ~25%.

SINGLE-CAVITY TESTS

Energy Gain Measurements

A 5.1-GHz standing-wave cavity, powered by a single HEMT at various power levels, was used to modulate (at low power) and accelerate (at higher power) an incoming 20-kV DC electron beam. The deflection of the beam in a dipole spectrometer is proportional to the beam momentum, allowing measurement of the energy gain delivered to the beam as a function of cavity power (Fig. 3) [4].

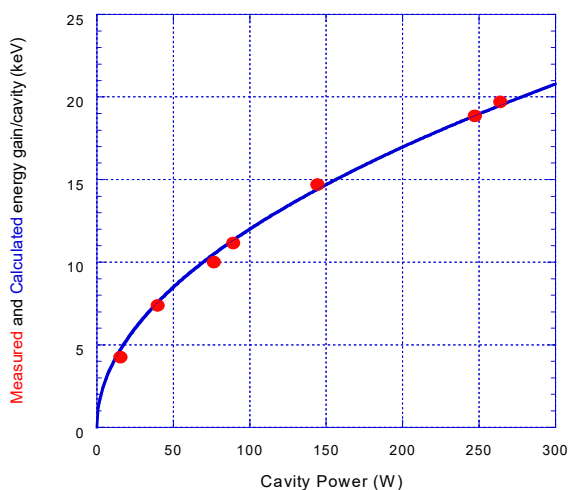


Figure 3: Plots of measured (red circles) and calculated energy gain (blue) as functions of cavity power.

Calorimetric Measurements

We measured the temperature rise in a C-band cavity operating with peak RF power of ~170 W (average power of 8.5 W at 5% and 17 W at 10% duty) without cooling and extracted from these measurements the average RF power absorbed by the cavity (Fig 4). The average rate of heat entering the cavity is the sum of the heat capacity and the heat conduction loss as given by

$$\dot{Q} = mC_v\dot{\theta} + \frac{\theta}{R_T} \quad (2)$$

where θ is the temperature rise, $\theta = T - T_{initial}$, m is the copper cavity mass, C_v is copper heat capacity and R_T is the thermal resistance. The latter can be calculated from measuring the temperature decay curve and extracting the thermal decay time constant τ , defined as $\tau = mC_vR_T$.

From the second temperature decay curve, the thermal time constant is 3.6 hours and the calculated average power delivered to the cavity agrees with the measured peak power of 170 W at 5% and 10% duty factor (Fig. 4).

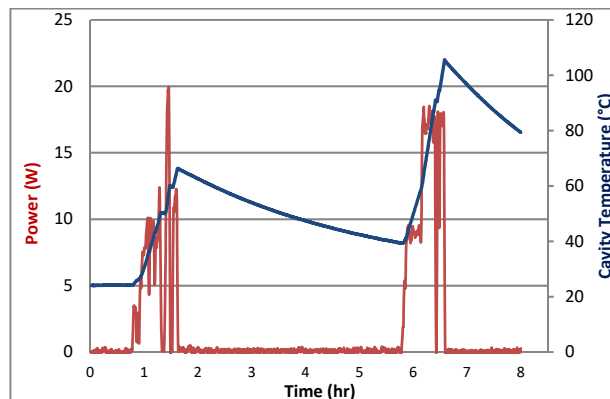


Figure 4: Plots of average power delivered to the cavity (red) and cavity temperature (blue) as functions of time.

Temperature-induced Frequency Shifts

We tracked the resonant frequency of a C-band cavity powered with 170 W at 5% and 10% duty factors without water cooling. As the cavity temperature rose by 65°C in 48 minutes, its resonant frequency decreased by 5.7 MHz (-88 kHz/°C) at a rate of 2 kHz/sec. We have designed a piezo tuner that will be inserted into the cavity to compensate for the temperature-induced frequency shifts.

TEN-CAVITY PROTOTYPE

Cavity Design Optimization

Using genetic algorithm, we have optimized the cavity shapes to maximize the shunt impedance for beam β of 0.2-0.7 (beam voltage of 10-200 keV). From the plot of shunt impedance versus beam β (Fig. 5), the best cavity β is about 0.4 in order to accelerate the sub-relativistic electrons in the first few cavities.

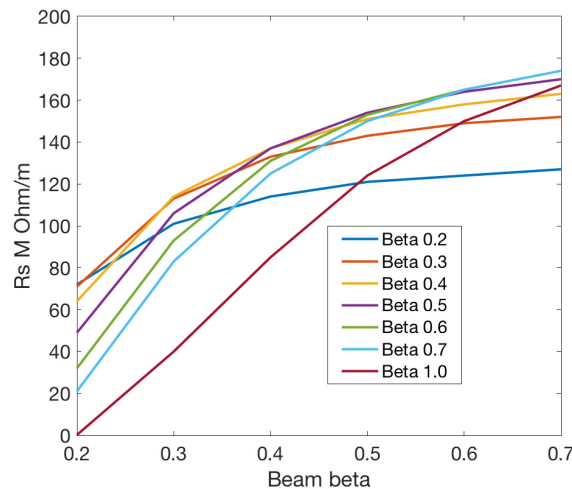


Figure 5: Plots of optimized cavity shunt impedance as functions of beam β . The $\beta = 0.4$ cavity provides the highest shunt impedance averaged over a wide range of β .

Content from this work may be used under the terms of the CC BY 3.0 licence (© 2018). Any distribution of this work must maintain attribution to the author(s), title of the work, publisher, and DOI.

Cavity Fabrication

The ten-cavity prototype has been fabricated by SLAC (Fig. 6a) and delivered to LANL for testing. A cross-section drawing of the $\beta=0.4$ cavity with the loop coupler and piezo frequency tuner is shown in Fig. 6b.

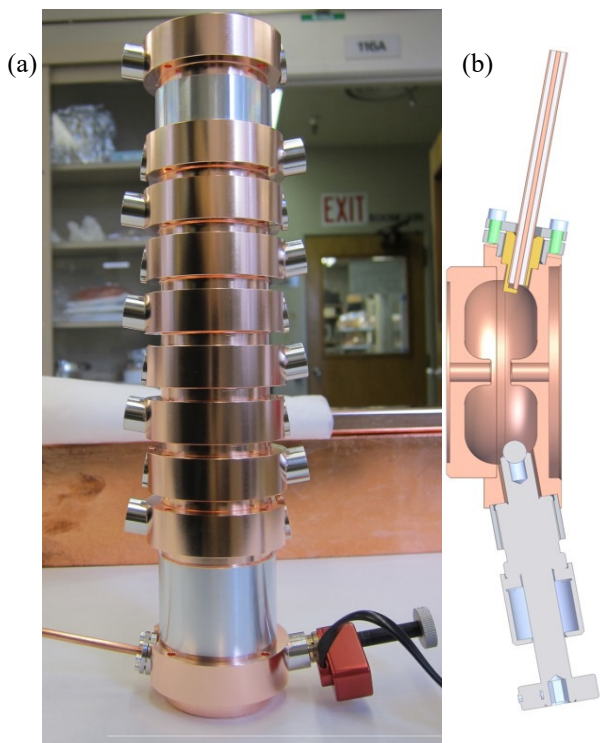


Figure 6: (a) Photo of the ten-cavity prototype; (b) cross-section drawing of the $\beta=0.4$ optimized cavity with the loop coupler (top) and piezo frequency tuner (bottom).

Beam Dynamics Simulations

Beam dynamics calculations were performed using the GPT beam simulation code. For these simulations, we select 50% of the electrons from the DC gun and accelerate them up to ~ 190 keV through the ten-cavity prototype. The ten cavities are physically independent and are controlled separately by their own LLRF systems, so we may explore the use of the first cell as a buncher cavity to improve beam capture, as well as the placement of focusing solenoids along the linac. For transverse focusing, we use two solenoids, one located between the 1st and 2nd cavity, and the other between the 5th and 6th cavities. Figure 7a plots the beam radius versus time after the beam exits the electron gun, showing the beam radius is focused to less than 0.5 mm for all cavities except the buncher cavity. Figure 7b shows the electron beam energy modulation in the first cavity and subsequent beam bunching after a drift distance between the 1st and 2nd cavities. This is possible because we can position the cavities independently from one another, a unique feature of the individually driven, HEMT-powered accelerator concept.

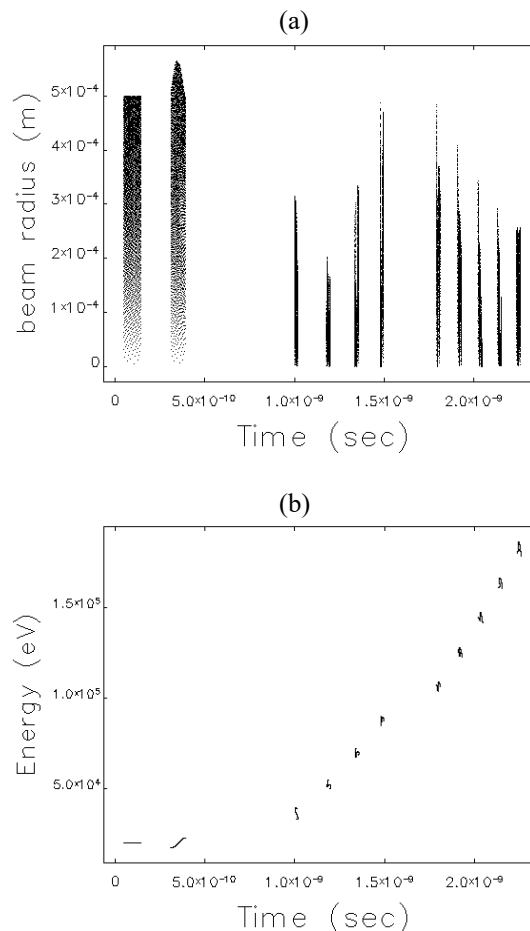


Figure 7: Plots of beam radius (a) and beam energy (b) versus time after exiting the electron gun.

SUMMARY & FUTURE PLAN

We are driving individual C-band cavities with 500-W, quasi-CW GaN high-electron mobility transistors. HEMT-driven C-band accelerator cavities can achieve mA average current and 25% wall-plug efficiency. Initial test results show energy gain per cavity of ~ 20 keV with ~ 260 W of RF power from a GaN C-band HEMT. SLAC and LANL are collaborating to test the ten-cavity prototype to demonstrate continuous energy gain in an all-solid-state HEMT-driven linac configuration. It will be mounted on a water-cooled breadboard to limit the rate of temperature rise during the initial testing of the piezo tuners that will be used for active frequency tracking.

ACKNOWLEDGMENTS

Research presented in this work is supported by (LANL) Laboratory Directed Research and Development 20170521ER and by (SLAC) Department of Energy contract DE-AC02-76SF00515. We appreciate the continuing support from Eric Dors, Bruce Carlsten, Duncan Mcbranch, Stephen Milton, and Paul Wantuck (LANL). We thank Elizabeth MacDonald and Jean-Marie Lauenstein (NASA Goddard Flight Center) and Ennio Sanchez (SRI International) for helpful discussions.

REFERENCES

- [1] For S-band, see <https://www.wolfspeed.com/cghv31500f>
for C-band see <http://www.wolfspeed.com/cghv59350>
for X-band see <https://www.wolfspeed.com/cghv96100f2>
- [2] J.W. Lewellen *et al.*, “Spaceborne Electron Accelerators,”
in Proc. LINAC’16, Lansing, MI, September 2016, paper
MO3A03, pp. 32-37.
- [3] B. Whelan *et al.*, *Med. Phys.* 43 (3), 2016, pp. 1285-1294.
- [4] J.W. Lewellen *et al.*, presented at IPAC’18, Vancouver,
Canada, April-May 2018, paper THPMF090, this confer-
ence.